

**CO-DELIVERY OF PACLITAXEL AND IMATINIB BY PEG DERIVATIZED NLG
CARRIER AS ENHANCED IMMUNOCHEMOTHERAPY**

by

Yuan Wei

BE Pharmaceutical Preparation, East China University of Science & Technology 2014

Submitted to the Graduate Faculty of
School of Pharmacy in partial fulfillment
of the requirements for the degree of
Master of Science

University of Pittsburgh
2016

UNIVERSITY OF PITTSBURGH
SCHOOL OF PHARMACY

This thesis was presented

by

Yuan Wei

It was defended on

May 17th, 2016

and approved by

Song Li, Professor, Pharmaceutical Science

Jiang Li, Research Associate Professor, Pharmaceutical Science

Vinayak Sant, Assistant Professor, Pharmaceutical Science

[Thesis Director/Dissertation Advisor]: Song Li, Professor, Pharmaceutical Science

Copyright © by Yuan Wei
2016

CO-DELIVERY OF PACLITAXEL AND IMATINIB BY PEG DERIVATIZED NLG CARRIER AS ENHANCED IMMUNOCHEMOTHERAPY

Yuan Wei, BE

University of Pittsburgh, 2016

Indoleamine 2,3-dioxygenase (IDO), which catalyzes the initial and rate-limiting step in the tryptophan catabolism along the kynurenine pathway, is an immunosuppressive enzyme that can lead to T cell anergy, apoptosis and potential induction of regulatory T cells (T_{reg} cells). This discovery has led to the development of several IDO inhibitors including NLG919, an immunotherapy drug that targets IDO with high efficacy, into the clinical trial for treating solid tumor. Our goal is to develop PEG derivatized NLG as a functional carrier for specifically delivering anticancer agents to the tumor site to stimulate immune response and eliminate systemic toxicity. Previously, our group has developed a PEG_{2K}-Fmoc-NLG micellar system that can effectively deliver anticancer drug Paclitaxel (PTX) and synergize with chemotherapy to reduce tumor growth. One major limitation with this approach is the feedback mechanism following NLG-mediated inhibition of IDO, which subsequently leads to the up-regulation of IDO expression. In addition, the mRNA expression of IDO can be further enhanced by PTX treatment. For long-term treatment, increased dose of this formulation would be necessary to maintain the same effect for treating cancer. The focus of our study is to identify a compound that can effectively inhibit the expression of IDO at transcriptional level and develop an improved PEG-NLG-based carrier for codelivery of the compound and a chemotherapeutic agent such as PTX.

In this thesis, the first aim was to examine the effect on IDO expression by several anticancer drug treatments. qRT-PCR analysis results show that several anticancer drugs including Paclitaxel, Doxorubicin and Dasatinib can up-regulate IDO expression while Imatinib (Gleevec®) exhibits the opposite effect. The second aim was to synthesize PEG_{5K}-(Fmoc-NLG)₂ as an improved dual functional carrier for co-delivery of Paclitaxel and Imatinib. PEG_{5K}-(Fmoc-NLG)₂ was successfully synthesized through 6 steps. The product at each step was confirmed by NMR. The third aim was focused on the characterization of our micellar system and the fourth aim was to examine the *in vivo* therapeutic efficacy.

TABLE OF CONTENTS

1. INTRODUCTION.....	1
1.1 Limitations of current anticancer drugs and effective drug delivery system for cancer treatment.	1
1.2 Stimulated immune response by conventional chemotherapy.	2
1.3 Immune checkpoints modulate immune escape during cancer progression.....	2
1.4 Indoleamine-2,3-dioxygenase (IDO) can be used as one therapeutic target to enhance immune response.....	3
1.5 PEG-Fmoc-NLG conjugates as dual-function carriers for cancer targeted delivery.....	4
1.6 IDO expression inhibitor can work synergistically with PEG detrivatised NLG based micellar system.	4
1.7 Overview of thesis.	6
2. MATERIALS AND METHODS	7
2.1 Materials	7
2.2 Cell Culture	7
2.3 qRT-PCR	8
2.4 Cytotoxicity Assay.....	8
2.5 Critical Micelle Concentration (CMC)	9
2.6 Kynurenine Inhibition Measurement Assay	9
2.7 Animals	10

2.8 Synthesis of PEG _{5k} -(Fmoc-NLG) ₂	10
3. RESULTS	13
3.1 Treatment by Anticancer Drugs on IDO Expression.	13
3.2 Combination Treatment of PTX and IMA on IDO Expression.	14
3.3 Combinational Treatment of PTX and IMA on Cancer Cell Growth.	15
3.4 Synthesis of PEG _{5k} -(Fmoc-NLG) ₂ Conjugate.	16
3.5 Characterization of Drug-Loaded PEG _{5k} -(Fmoc-NLG) ₂ Micelles.	17
3.5.1 Size Distribution and Morphology of Free Drug PEG _{5k} -(Fmoc-NLG) ₂ Micelles, PTX loaded Micelles and PTX, IMA Co-loaded Micelles.	17
3.5.2 Stability Investigation of PEG _{5k} -(Fmoc-NLG) ₂ Micelles.	19
3.5.3 Critical Micellar Concentration (CMC) of PEG _{5k} -(Fmoc-NLG) ₂ Micellar System.	20
3.5.4 Kynurenine Inhibition Measurement of PEG _{5k} -(Fmoc-NLG) ₂ Conjugate... ..	21
3.5.5 <i>In Vitro</i> Cytotoxicity of Drug-loaded PEG _{5k} -(Fmoc-NLG) ₂ Micelles.....	22
3.6 <i>In Vivo</i> Therapeutic Study	23
3.7 RT-PCR Analysis of IDO Transcripts from tumor tissues.	26
4. DISCUSSION	28
BIBLIOGRAPHY	30

LIST OF TABLES

Table 1. Physicochemical characterization of drug-loaded PEG _{5k} -(Fmoc-NLG) ₂ micellar system.	20
---	----

LIST OF FIGURES

Figure 1. Overview of PEG _{5k} -(Fmoc-NLG) ₂ conjugate as improved carrier for co-delivery of Paclitaxel and Imatinib.	6
Figure 2. Synthesis scheme of PEG _{5k} -(Fmoc-NLG) ₂ conjugate.	10
Figure 3. qRT-PCR analysis showing IDO expression of 4T1.2 cell treated with different anti-cancer agents including (A) PTX, (B) PTX plus ifn- γ , (C) IMA and (D) IMA plus ifn- γ , (E) DOX and (F) DAS. n= 3-4 each, significance determined by one-way ANOVA with Tukey's post hoc test; p* $<$ 0.05, p** $<$ 0.01. All values are mean \pm Standard Deviation.	14
Figure 4. qRT-PCR analysis showing IDO expression of 4T1.2 cell treated with combination of PTX and IMA with (A) and without (B) ifn- γ induction. Concentration of ifn- γ = 50ng/ml. n= 3-4 each, significance determined by one-way ANOVA with Tukey's post hoc test; p* $<$ 0.05, p** $<$ 0.01. All values are mean \pm Standard Deviation.	15
Figure 5. Cytotoxicity of PTX and IMA combinational treatment on 4T1.2 cell line showing no synergistic effect between these two anti-cancer agents. The experiment were repeated four times. Results are showing in mean \pm Standard Deviation.	16
Figure 6. ¹ H-NMR of PEG _{5k} -(Fmoc-NLG) ₂ conjugate	17
Figure 7. (A,B) Size distribution and morphology of free drug PEG _{5k} -(Fmoc-NLG) ₂ micelles; (C,D) PTX-loaded PEG _{5k} -(Fmoc-NLG) ₂ micelles; (E,F) PTX+IMA-loaded PEG _{5k} -(Fmoc-NLG) ₂ micelles;	18
Figure 8. Critical micelle concentration (CMC) of PEG _{5k} -(Fmoc-NLG) ₂ micelle.	21

Figure 9. NLG and PEG_{5k}-(Fmoc-NLG)₂ conjugate potently inhibit kynurenine production at a dose-dependent manner in ifn- γ -treated Hela cells. Concentration of ifn- γ = 50 ng/mL. The experiment was performed in triplicate and all values are mean \pm Standard Deviation..... 22

Figure 10. Cytotoxicity of PTX-loaded PEG_{5k}-(Fmoc-NLG)₂, IMA-loaded PEG_{5k}-(Fmoc-NLG)₂ and PTX+IMA-loaded PEG_{5k}-(Fmoc-NLG)₂ micelles in comparison to Taxol formulation in various types of tumor cells including (A) 4T1.2, (B) PANC-2, (C) MCF-7 and (D) PC-3. The experiment was performed in triplicate and all values are mean \pm Standard Deviation..... 23

Figure 11. (A) *In vivo* therapeutic study of drug free PEG_{5k}-(Fmoc-NLG)₂, PTX-loaded PEG_{5k}-(Fmoc-NLG)₂, IMA-loaded PEG_{5k}-(Fmoc-NLG)₂ and PTX+IMA-loaded PEG_{5k}-(Fmoc-NLG)₂ micelles in comparison to Taxol formulation on 4T1.2 bearing BALB/c mice model. n=4-5 each group. Injection was given on day 0, 2, 4, 7 and 10 respectively. (B) Changes of body weight in mice that received different treatments. (C) Observation of tumor size from each group. (D) Average tumor weight from each group. Significance determined by one-way ANOVA with Fisher's post hoc test; p*<0.05, p**<0.01, p***<0.001. All values are mean \pm S.E.M..... 26

Figure 12. qRT-PCR analysis showing IDO mRNA from mouse 4T1.2 tumor tissues (n=4-5 each group). All values are mean \pm S.E.M 27

1. INTRODUCTION

1.1 Limitations of current anticancer drugs and effective drug delivery system for cancer treatment.

Chemotherapy, designed to use drugs directly kill cancer cells, is one of the major approaches to treat cancer. It can be used alone or in the combination with several other forms of therapy. Paclitaxel (PTX) is one of the first-line chemo drugs for treatment of ovarian, breast, lung, pancreatic and other cancers. However, clinical application of PTX has been suffered from low aqueous solubility, rapid elimination and lack of selectivity.¹ Taxol is a Cremophor EL/ethanol formulation of PTX that has been used in clinic. But Cremophor EL can cause hyperactivity reaction, neuropathy and many other severe side effects. For these reasons, it is necessary to develop an alternative delivery system not only to defeat these limitations but also increase the potency of anticancer agents. Micelle, one of the nanocarriers, is an aggregate of amphiphilic molecules dispersed in the aqueous solution.² A typical micelle has a hydrophilic head outside and hydrophobic tail regions inside the structure. Polyethylene glycol (PEG) is a safe, non-toxic, highly hydrated and biodegradable polymer with many applications in medicine, which can also be utilized as classic hydrophilic head of the micellar system. The incorporation of chemo drugs into micellar systems has several advantages such as relatively small size (10-100nm),³ increased bioavailability and passively targeted to the tumor sites by the enhanced permeability and retention (EPR) effect.^{4,5} The hydrophilic shell of the PEG-derivatized micellar system provides steric stability by preventing the recognition and binding of plasma protein, further avoiding uptake by the reticuloendothelial system

(RES).³ In addition, the versatility of PEG-derivatized micellar system can be utilized as a platform for a broad range of chemo drugs with different structures.

1.2 Stimulated immune response by conventional chemotherapy.

Generally, most chemo drugs lead to death of all fast dividing cells including both tumor cells and healthy cells. However, accumulating evidence indicates that chemo drug can stimulate the host immune system that cooperates for successful tumor elimination.^{6,7} In response to chemotherapy, the dying tumor cells will expose Calreticulin (CRT) on the outer leaflet of their plasma membrane at a preapoptotic stage, secret Adenosine Triphosphate (ATP) during apoptosis and release nuclear protein high-mobility group box 1 (HMGB1) to facilitate the activation of dendritic cells (DCs) and T cells to further induce cytotoxic T cells to kill tumor cells.⁸

1.3 Immune checkpoints modulate immune escape during cancer progression.

Although chemotherapy can stimulate immune response, such response exhibits some limitations; one of them is due to the immune checkpoints. The immune checkpoints are negative regulators of the immune system. Normally, they paly critical roles in maintaining self-tolerance and protecting tissues from immune collateral damage when the immune system responses to pathogenic infection.⁹ These immune checkpoints can also be co-opted by tumor cells to escape from the immune destruction. Blocking those immune checkpoints is thus a promising approach to enhance anti-tumor immunity. There are several immune checkpoints that have been actively studies to the context of clinical cancer immunotherapy, including cytotoxic T-lymphocyte-associated antigen 4

(CTLA4), programmed cell death protein 1 (PD-1) and Indoleamine-2,3-dioxygenase (IDO).¹⁰ They can regulate immune response at different levels with different mechanisms. Because both the role of CTLA4 and PD-1 are initiated by ligand-receptor interactions, they can be readily blocked by antibodies.^{11,12} CTLA4 antibody Ipilimumab (Yevoy[®]) and PD-1 antibodies Nivolumab (Opdivo[®]) and Iambrolizumab (Keytruda[®]) have been approved by US Food and Drug and Administration (FDA).

1.4 Indoleamine-2,3-dioxygenase (IDO) can be used as one therapeutic target to enhance immune response.

Indoleamine-2,3-dioxygenase (IDO) is the initial and rate-limiting enzyme of tryptophan catabolism along the kynurenine pathway.¹³ Initially the role of IDO was thought to be mainly antimicrobial by reducing the availability of the essential amino acid tryptophan in the inflammatory environment.¹⁴⁻¹⁶ The earliest studies of IDO related to cancer were made in 1950s that researchers observed tryptophan catabolites are elevated in cancer patients. Next a groundbreaking discover work was done in 1998 by Munn's group.^{17,18} Their study, for the first time, showed that IDO might mediate immunosuppression based on the preferential sensitivity of T cells to tryptophan deprivation. IDO is overexpressed by antigen presenting cells in many cancers. Its activity leads to the deficiency of local tryptophan and production of tryptophan metabolites, such as kynurenine, which have been shown to have immunosuppression effects including promoting T_{reg} cell differentiation, blocking T-lymphocyte proliferation, suppressing immune response and decreasing Dendritic cell (DC) function.^{19,20} Several studies also showed that IDO can be induced by ifn- γ , an inflammatory cytokine, through JAK-STAT signaling pathway.²¹

Therefore, a number of chemicals and other small molecules have been developed to act as IDO inhibitors. NLG919 (NLG), a potent specific enzymatic inhibitor of IDO, is already in the clinical Phase I trial.²²

1.5 PEG-Fmoc-NLG conjugates as dual-function carriers for cancer targeted delivery.

9-fluorenylmethoxycarbonyl (Fmoc) moiety, a functional group routinely used for amino acid protection, was demonstrated as one of the most potent drug-interactive motif. The incorporation of Fmoc motif into PEG-drug conjugates can increase both the drug-loading capacity and formulation stability.^{23,24} Previously, a PEG_{2k}-Fmoc-NLG conjugate was developed by our group, which can work as a functional carrier to deliver anticancer drug Paclitaxel (PTX) specifically to the tumor site. Meanwhile, the release of NLG can inhibit the activity of IDO and help to re-establish an immunogenic response to cancer. *In vivo* study in a 4T1.2 murine breast cancer tumor model has shown enhanced effect of chemotherapy to reduce tumor growth compared with commercial formulation Taxol[®].

1.6 IDO expression inhibitor can work synergistically with PEG detritivatised NLG based micellar system.

Although PTX-loaded PEG_{2k}-Fmoc-NLG micelles showed enhanced antitumor activity, we found out both the carrier and PTX-loaded micelles induced an up-regulation of IDO expression at the mRNA level. We believe this is due to the negative feedback mechanism. NLG is known as an enzymatic inhibitor of IDO. Thus, decrease in the

amount of enzymatic metabolites would cause an increase in the expression of the enzyme. For long-term treatment, increased dose of this formulation would be necessary to maintain the same effect for treating cancer. , PTX could also induce the $\text{ifn-}\gamma$, which, in turn, leads to further induction of IDO. Imatinib is the first generation Bcr-Abl tyrosine kinase inhibitor mainly used to treat chronic myelogenous leukemia (CML).²⁵⁻²⁷ A recent study reported that Imatinib showed an inhibitory effect on IDO expression, which potentiates antitumor T cell response in gastrointestinal stromal tumor (GIST).²⁶ We hypothesized that addition of Imatinib into our current combination protocol shall represent a more effective immunochemotherapy via inhibiting IDO at both transcriptional and enzymatic levels.

1.7 Overview of thesis.

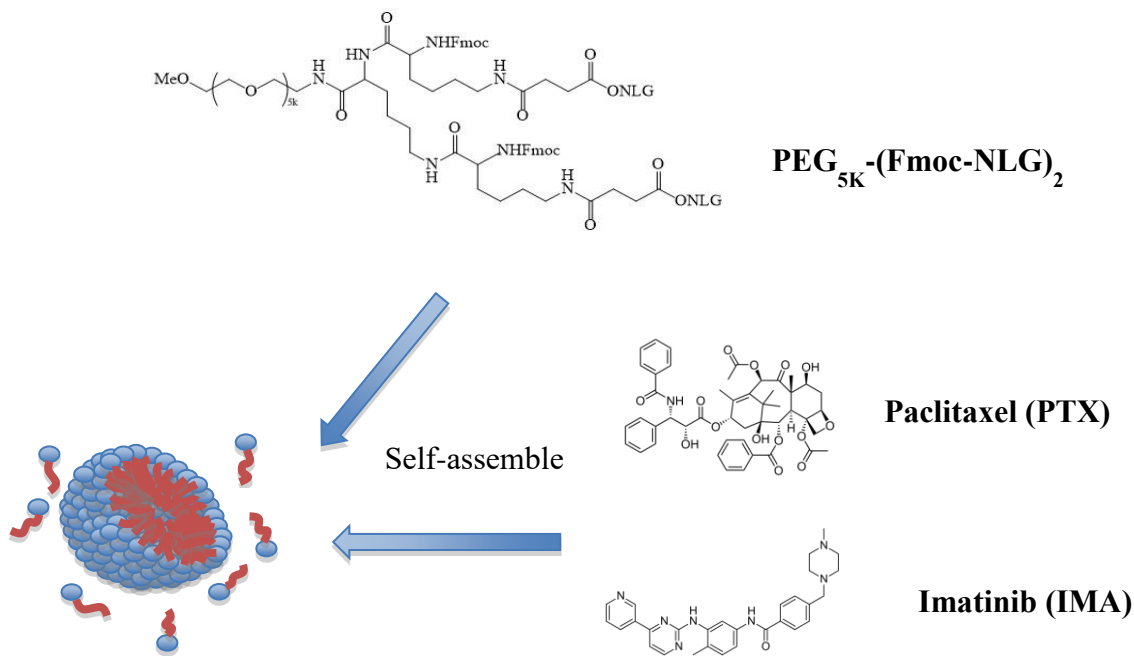


Figure 1. Overview of PEG_{5K}-(Fmoc-NLG)₂ conjugate as improved carrier for co-delivery of Paclitaxel and Imatinib.

Hence, in this thesis, we first examined the effect on IDO expression by several anticancer drug treatments in cancer cell lines and confirmed the down-regulation effect of Imatinib on IDO expression. Secondly, we successfully synthesized an improved PEG-NLG-based carrier, PEG_{5K}-(Fmoc-NLG)₂ for co-delivery of PTX and IMA. Finally, the new micellar system was extensively characterized with respect to both biophysical properties and the therapeutic efficacy in a murine breast cancer model (4T1.2).

2. MATERIALS AND METHODS

2.1 Materials

Poly(ethylene glycol) methyl ether (MeO–PEG–OH, MW = 5000 kDa), dichloromethane (DCM), Dimethyl sulfoxide (DMSO), 3-(4,5-dimethylthiazol-2-yl)-2,5-diphenyl tetrazolium bromide (MTT), Nile Red, p-dimethylamino benzaldehyde, trichloroacetic acid (TCA), Acetic Acid and Dulbecco's Modified Eagle's Medium (DMEM) were all purchased from Sigma-Aldrich (MO, U.S.A). Boc-Lys(Boc)-OH and Fmoc-Lys(Boc)-OH were purchased from GL Biochem (Shanghai, China). Succinic Anhydride was purchased from TCI AMERICA (OR, USA). Dicyclohexylcarbodiimide (DCC) and Trifluoroacetic Acid (CF₃COOH) were purchased from Alfa Aesar (MA, USA). 4-(dimethylamino) pyridine (DMAP) was purchased from Calbiochem-Novabiochem Corporation (CA, USA). Triethylamine (TEA) was purchased from Acros Organic (NJ, USA). Fetal bovine serum (FBS) and penicillin–streptomycin solution were purchased from Invitrogen (NY, USA). TRIzol Reagent was purchased from life technologies (CA, USA). All solvents used in this study were HPLC grade.

2.2 Cell Culture

Hela is a human cervical cancer cell line. MCF-7 is a human breast carcinoma cell line. PC-3 is a human prostate cancer cell lines. 4T1.2 is a mouse metastatic breast cancer cell line and PANC-2 is a mouse pancreatic cancer cell line. All cell lines were cultured in DMEM containing 10% FBS and 1% penicillin–streptomycin at 37 °C in a humidified 5% CO₂ atmosphere.

2.3 qRT-PCR

For in vitro investigation, 4T1.2 cell (15000 cells/well) were seeded in 6-well plates followed by 24 h of incubation in DMEM with 10% FBS and 1% streptomycin/penicillin. Then, various concentration of free PTX, IMA, Doxorubicin (DOX), Dasatinib (DAS) and the combination of PTX and IMA respectively were added and cells were incubated in DMEM with 2% FBS and 1% streptomycin/penicillin for 16~20h. Next we extracted total RNA, reverse-transcribed using High-Capacity cDNA Reverse Transcription Kit purchased from Thermo Fisher (MA, USA) and amplified cDNA with PCR SYBR Green probes for mouse genes encoding ifn- γ , IDO and GAPDH (Eurofins, Luxembourg).

2.4 Cytotoxicity Assay

MCF-7 (4000 cells/well), PC-3 (2000 cells/well), 4T1.2 (1000 cells/well) and PANC-2 (1000 cells/well) were seeded in 96-well plates followed by 24 h of incubation in DMEM with 10% FBS and 1% streptomycin/penicillin. Then, various concentrations of free PTX or free IMA and the combination of both respectively were added in triplicate and cells were incubated in DMEM with 2% FBS and 1% streptomycin/penicillin for 72 h. After removing the medium in the plates, 100 μ L of 3-(4, 5-dimethylthiazol-2-yl)-2,5-diphenyltetrazoliumbromide (MTT) in 0.9% Saline was added and cells were further incubated for 4 h. After removing the medium in the plates, MTT formazan was solubilized by DMSO. The absorbance of each well was measured by the microplate-reader, with wavelength at 550 nm and reference wavelength at 630 nm. Untreated

groups were served as controls. Cell viability was calculated as $[(OD_{\text{treat}} - OD_{\text{blank}})/(OD_{\text{control}} - OD_{\text{blank}}) \times 100\%]$. Same assay was also applied for micelles (Carrier, PTX/Carrier, IMA/Carrier, PTX+IMA/Carrier and Taxol) cytotoxicity test on these cell lines.

2.5 Critical Micelle Concentration (CMC)

The CMC of PEG_{5k}-(Fmoc-NLG)₂ micelles were measured using Nile red as a fluorescence probe with final concentration of 1.25nM. Nile red fluorescence was measured at 25°C using an excitation wavelength between 490 and 590 nm. Fluorescent emission was measured from 550 to 700nm at 5 nm intervals.²⁸

2.6 Kynurenine Inhibition Measurement Assay

Hela (2000 cells/well) were seeded in 96-well plates followed by 24 h of incubation in DMEM with 10% FBS and 1% streptomycin/penicillin. Then, various concentration of NLG or PEG_{5k}-(Fmoc-NLG)₂ were added to the cell together with ifn- γ (50ng/mL) for 2 days. Next, we collect 100 μ L of the cell culture supernatant and add 50 μ L 30% w/v trichloroacetic acid (TCA) and incubated for 40 min at 50°C to hydrolyze N-formylkynurenine to kynurenine. After centrifugation at 3000 rpm for 10 min, 100 μ L of the supernatant were transferred into a new 96-well plate and mixed with 100 μ L 2% w/v p-dimethylamino benzaldehyde in 99/8% v/v acetic acid. After incubation for 10 min at room temperature. Kynurenine was detected by measuring the absorbance at 490nm. The absorbance of the culture medium alone without any treatment was considered as blank.²⁸

DMAP (37mg, 0.3 mmol, 0.3 eq) were dissolved in DCM and stirred at room temperature for two days. The mixture was filtered through cotton and then purified through two cycles of dissolution/reprecipitation with DCM/ether and DCM/ethanol respectively to afford MeO-PEG_{5k}-di-Boc-lysine (4.5 g, 0.8 mmol, 84% yield).

Step 2: Preparation of MeO-PEG_{5k}-lysine-(NH₂)₂

MeO-PEG_{5k}-di-Boc-lysine (4.5g, 0.87 mmol) was dissolved in 20 mL mixture of trifluoroacetic acid (TFA) (50% in volume)/DCM. The mixture was stirred for 2 hours at room temperature and purified through three cycles of dissolution/reprecipitation with DCM/ether to give MeO-PEG_{5k}-Boc-lysine-(NH₂)₂ (4.0 g, 0.8 mmol, 97% yield).

Step 3: Preparation of MeO-PEG_{5k}-lysine-Fmoc₂-di-Boc-lysine

MeO-PEG_{5k}-lysine-(NH₂)₂ (4.0 g, 0.8 mmol, 1.0 eq), Fmoc-Lys(Boc)-OH (2.12g, 4.8 mmol, 6.0 eq), DCC (0.93mg, 4.8mmol, 6.0 eq) and DMAP (27mg, 0.24 mmol, 0.3 eq) were dissolved in 20 mL DCM and stirred for 2 days at room temperature. The mixture was filtered through cotton and then purified through two cycles of dissolution/reprecipitation with DCM/ether and DCM/ethanol respectively to afford MeO-PEG_{5k}-lysine-Fmoc₂-di-Boc-lysine (3.8 g, 0.66 mmol, 91% yield).

Step 4: Preparation of MeO-PEG_{5k}-lysine-Fmoc₂-lysine-(NH₂)₂

MeO-PEG_{5k}-lysine-Fmoc₂-di-Boc-lysine was dissolved in 20 mL mixture of trifluoroacetic acid (TFA) (50% in volume)/DCM. The mixture was stirred for 2 hours at room temperature and purified through three cycles of dissolution/reprecipitation with

DCM/ether to give MeO-PEG_{5k}-lysine-Fmoc₂-lysine-(NH₂)₂ (3.5 g, 0.6 mmol, 90% yield).

Step 5: Preparation of MeO-PEG_{5k}-lysine-Fmoc₂-lysine-COOH₂

MeO-PEG_{5k}-lysine-Fmoc₂-lysine-(NH₂)₂ (3.5 g, 0.7 mmol, 1.0eq), succinic anhydride (240 mg, 2.8 mmol, 4.0 eq), DMAP (290 mg, 2.8 mmol, 4.0 eq) were dissolved in 20 mL DCM and stirred overnight at room temperature. The mixture was purified through two cycles of dissolution/reprecipitation with DCM/ether and DCM/ethanol respectively to afford MeO-PEG_{5k}-lysine-Fmoc₂-lysine-COOH₂ (3.0 g, 0.5 mmol, 85% yield).

Step 6: Preparation of PEG_{5k}-(Fmoc-NLG)₂

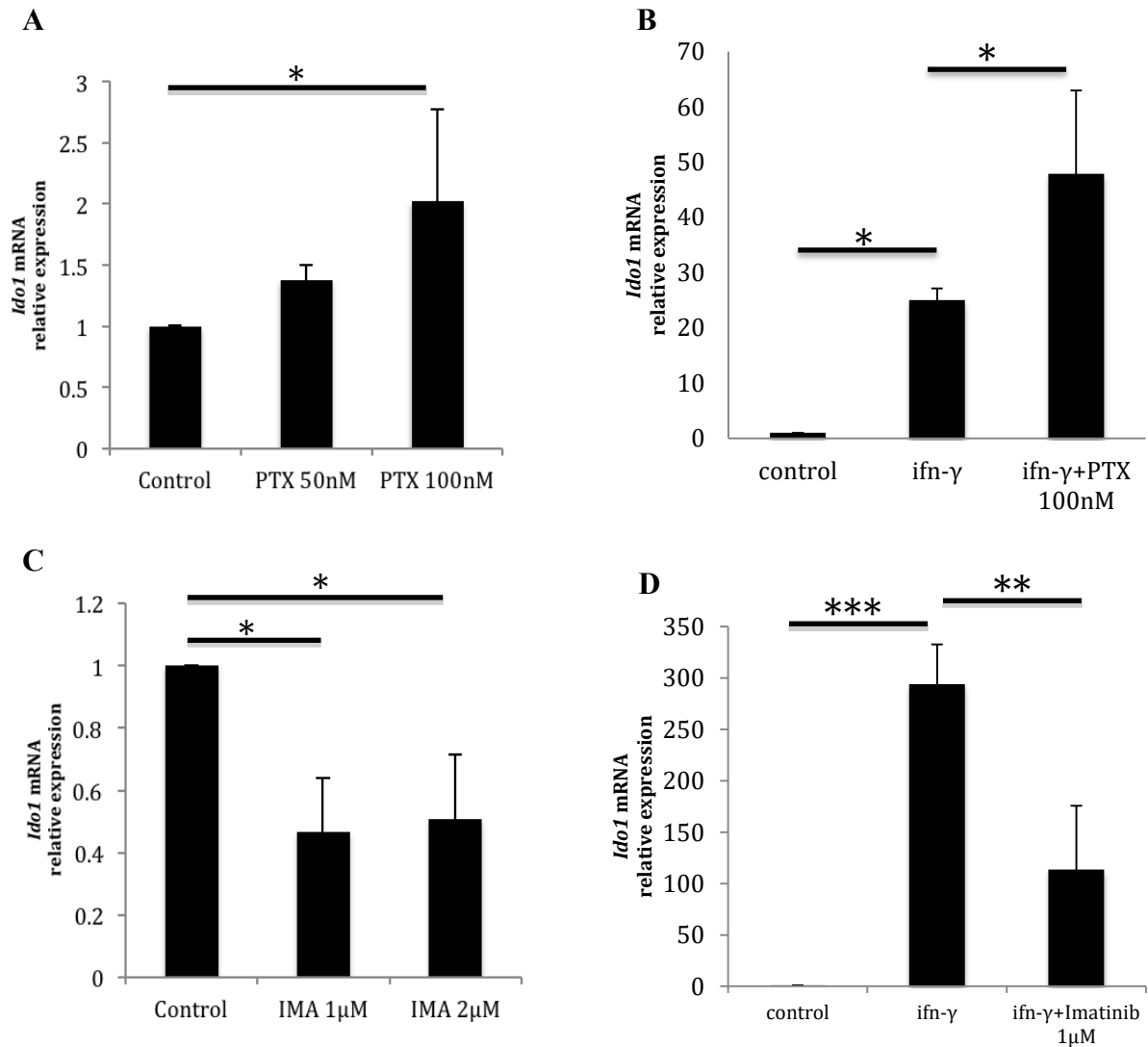
MeO-PEG_{5k}-lysine-Fmoc₂-lysine-COOH₂ (250mg, 0.0414mmol, 1.0eq), NLG919 (70mg, 0.24mmol, 6.0eq), DCC (51.2mg, 0.248mmol, 6.0eq), DMAP (5mg, 0.041mmol, 6.0eq) were dissolved in 1 mL DCM and stirred for 2 days at room temperature. The mixture was purified through two cycles of dissolution/reprecipitation with DCM/ether and DCM/ethanol respectively to afford PEG_{5k}-(Fmoc-NLG)₂ (200mg, 0.03mmol, 86% yeild)

3. RESULTS

3.1 Treatment by Anticancer Drugs on IDO Expression.

In consistent with previous reports²⁹, ifn- γ treatment led to a significant induction of IDO 1 mRNA expression (Fig. 3B). PTX treatment also showed a modest effect in inducing the IDO 1 expression (Fig. 3A) The combination of the two showed an effect that was more dramatic than the one with each treatment alone (Fig. 3B).

Dox or Das treatment also showed some effect in inducing the expression of IDO1 mRNA (Fig. 3E, F). In contrast, IMA treatment significantly inhibited both basal and IFN- γ induced IDO1 mRNA expression (Fig. 3C, D).



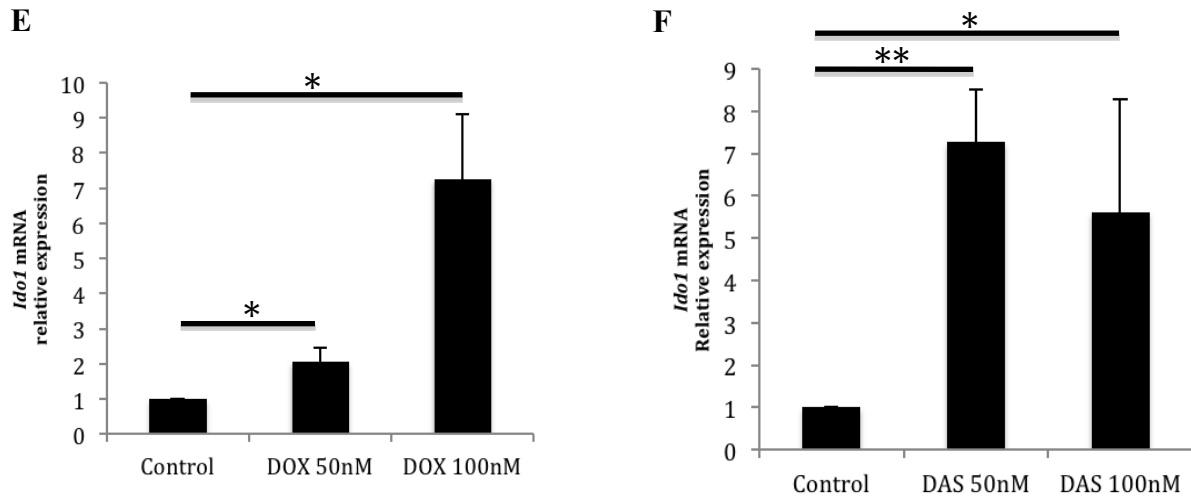


Figure 3. qRT-PCR analysis showing IDO expression of 4T1.2 cell treated with different anti-cancer agents including (A) PTX, (B) PTX plus ifn- γ , (C) IMA and (D) IMA plus ifn- γ , (E) DOX and (F) DAS. n= 3-4 each, significance determined by one-way ANOVA with Tukey's post hoc test; $p^* < 0.05$, $p^{**} < 0.01$. All values are mean \pm Standard Deviation.

3.2 Combination Treatment of PTX and IMA on IDO Expression.

After demonstrating the inhibitory effect of IMA on IDO1 expression, we then investigated whether IMA could also inhibit the PTX-induced IDO1 expression under both basal condition and stimulation by IFN- γ . In consistent with the data in Figure 3, PTX treatment led to significant induction of IDO1 mRNA, particularly in combination with IFN- γ . However this induction was significantly inhibited via co-treatment with IMA.

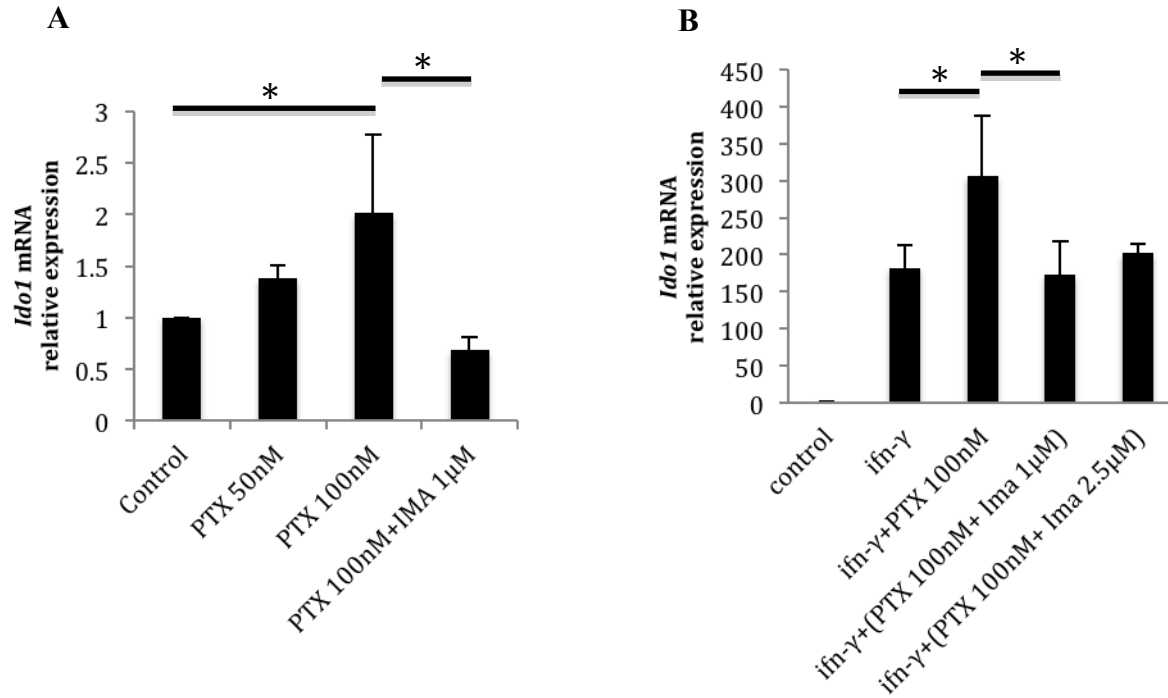


Figure 4. qRT-PCR analysis showing IDO expression of 4T1.2 cell treated with combination of PTX and IMA with (A) and without (B) ifn- γ induction. Concentration of ifn- γ = 50ng/ml. n= 3-4 each, significance determined by one-way ANOVA with Tukey's post hoc test; $p^* < 0.05$, $p^{**} < 0.01$. All values are mean \pm Standard Deviation.

3.3 Combinational Treatment of PTX and IMA on Cancer Cell Growth.

The cytotoxicity of PTX and IMA co-treatment effect was examined on 4T1.2 cell line. When the cell line was treated with PTX and IMA, there was a dose-dependent inhibition of cell proliferation. With fixed concentration of PTX, especially at the concentration below IC_{50} , addition of IMA did not lead to enhanced growth inhibition, suggesting lack of synergy between PTX and IMA on 4T1.2 tumor cells.

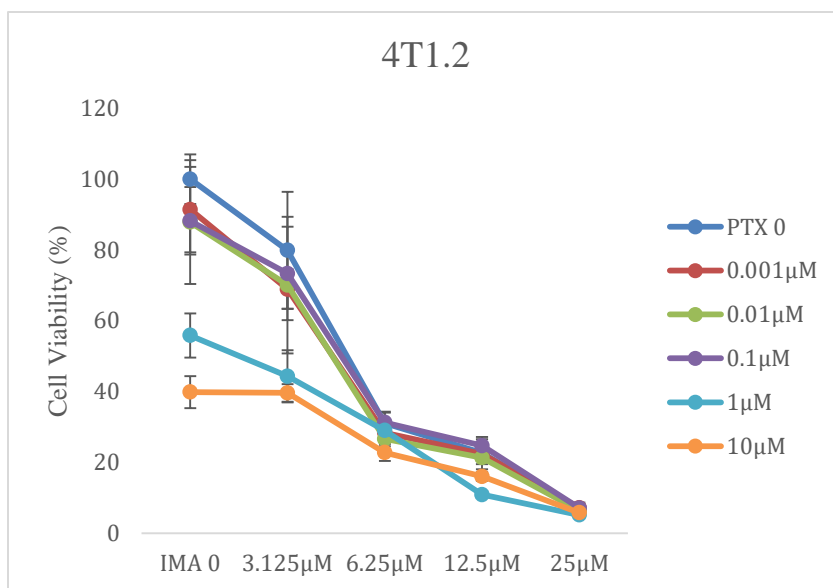


Figure 5. Cytotoxicity of PTX and IMA combinational treatment on 4T1.2 cell line showing no synergistic effect between these two anti-cancer agents. The experiment were repeated four times. Results are showing in mean \pm Standard Deviation.

3.4 Synthesis of PEG_{5k}-(Fmoc-NLG)₂ Conjugate.

Our previous carrier, PEG_{2k}-Fmoc-NLG was effective in delivery of PTX but was not capable of codelivery of PTX and IMA. We believed that this was likely due to the limited size of drug-interactive pocket. We hypothesized that a similar carrier with an expanded drug-interactive pocket such as PEG_{5k}-(Fmoc-NLG)₂ shall be more effective in co-formulating PTX and IMA. PEG_{5k}-(Fmoc-NLG)₂ was synthesized through 6 steps and ¹H-NMR spectrum is shown in Figure 6. Signals at 3.63 ppm are attributable to the methylene protons of PEG. Signals at 7-8 ppm are attributable benzene ring protons of Fmoc motif and protons of NLG. Signal at 5.3-5.4 ppm represents for the protons of NLG. Signals from 1 ppm to 1.5 ppm are attributable to the cyclohexane of NLG. These data suggest successful preparation of PEG_{5k}-(Fmoc-NLG)₂.

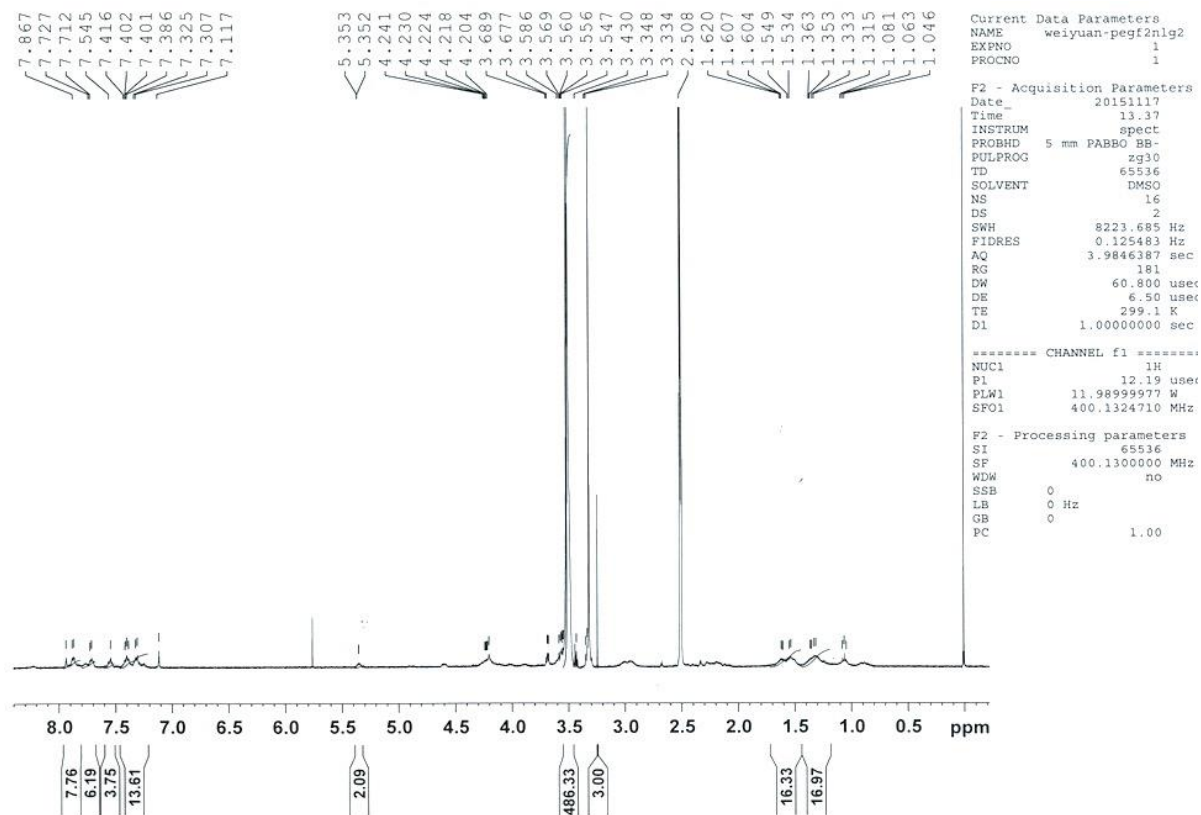


Figure 6. $^1\text{H-NMR}$ of $\text{PEG}_{5k}\text{-(Fmoc-NLG)}_2$ conjugate

3.5 Characterization of Drug-Loaded $\text{PEG}_{5k}\text{-(Fmoc-NLG)}_2$ Micelles.

3.5.1 Size Distribution and Morphology of Free Drug $\text{PEG}_{5k}\text{-(Fmoc-NLG)}_2$ Micelles, PTX loaded Micelles and PTX, IMA Co-loaded Micelles.

Our $\text{PEG}_{5k}\text{-(Fmoc-NLG)}_2$ conjugate can readily formed micelles in aqueous solution.

Dynamic light scattering (DLS) measurements showed that our micelles either carrier alone or loaded with drugs had hydrodynamic size around 100 to 120 nm. Transmission electron microscopy (TEM) image showed our micelles were spherical particles with a uniform size distribution.

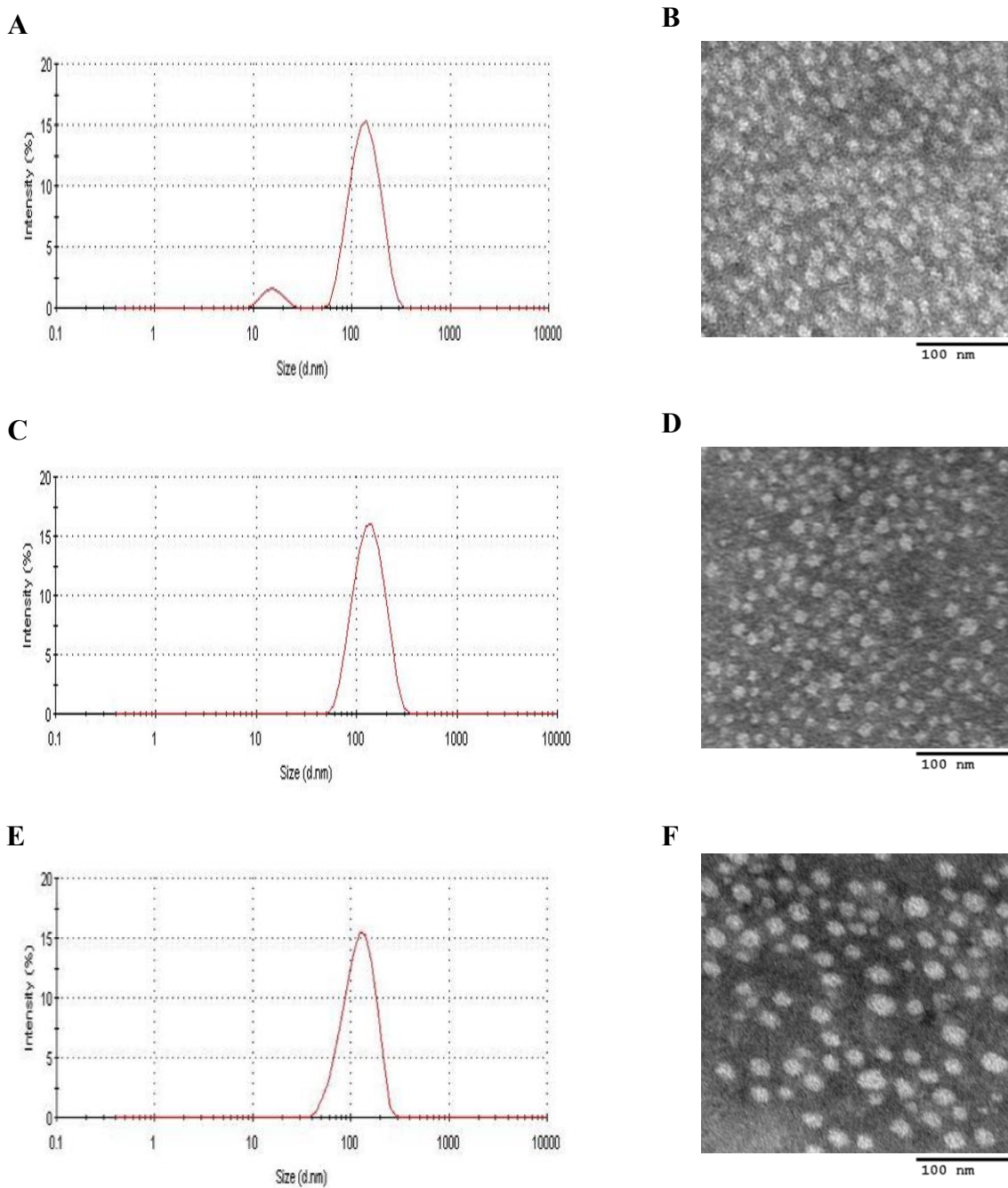


Figure 7. (A,B) Size distribution and morphology of free drug PEG_{5k}-(Fmoc-NLG)₂ micelles; (C,D) PTX-loaded PEG_{5k}-(Fmoc-NLG)₂ micelles; (E,F) PTX+IMA-loaded PEG_{5k}-(Fmoc-NLG)₂ micelles;

3.5.2 Stability Investigation of PEG_{5k}-(Fmoc-NLG)₂ Micelles.

A minimal carrier/drug ratio of 0.5:1 was required to load PTX into PEG_{5k}-(Fmoc-NLG)₂ micelles and the particles were stable for ~2 hour at room temperature and ~8 hour at 4°C. For loading of IMA, the minimal carrier/drug ratio was 1:1 and the particles were stable for about 1 day at room temperature. Increasing the carrier/drug ratio was associated with a significant improvement in the stability of drug-loaded micelles at both room temperature and 4°C. At a carrier to drug ratio of 5:1:1 molar ratio of carrier to drug can successfully load two drugs and stabilize for 60 hours. The detailed data on drug loading capacity and formulation stability are shown in table 1.

Micelles ^a	Molar	Stability	Stability	DLC ^b (%)	DLC (%)
	Ratio	(RT)	(4°C)	PTX	IMA
PEG _{5k} -(Fmoc-NLG) ₂ : PTX	0.5:1	6 h	12 h	20.8	--
PEG _{5k} -(Fmoc-NLG) ₂ : PTX	1:1	24 h	7 d	11.6	--
PEG _{5k} -(Fmoc-NLG) ₂ : PTX	2.5:1	2 d	40 d	5	--
PEG _{5k} -(Fmoc-NLG) ₂ : PTX	5:1	3 d	43 d	2.6	--
PEG _{5k} -(Fmoc-NLG) ₂ : IMA	1:1	18 h	5 d	--	7.3
PEG _{5k} -(Fmoc-NLG) ₂ : IMA	2.5:1	5 d	7 d	--	3.2
PEG _{5k} -(Fmoc-NLG) ₂ : IMA	5:1	14 d	36 d	--	1.5
PEG _{5k} -(Fmoc-NLG) ₂ : IMA: PTX	1:1:1	18 h	5 d	11	6.3
PEG _{5k} -(Fmoc-NLG) ₂ : IMA: PTX	2.5:1:1	24 h	14 d	4.9	2.8
PEG _{5k} -(Fmoc-NLG) ₂ : IMA: PTX	5:1:1	60 h	30 d	2.5	1.5

Table 1. Physicochemical characterization of drug-loaded PEG_{5k}-(Fmoc-NLG)₂ micellar system.

^a PTX concentration in micelles was kept at 1 mg/mL and IMA concentration in micelles was kept at 0.58 mg/mL. ^b DLC = drug loading capacity. $\text{DLC (\%)} = [\text{weight of drug loaded} / (\text{weight of polymer} + \text{drug used})] \times 100$

3.5.3 Critical Micellar Concentration (CMC) of PEG_{5k}-(Fmoc-NLG)₂ Micellar System.

CMC is defined as the concentration of surfactants above which micelles form. The CMC of PEG_{5k}-(Fmoc-NLG)₂ micelle was measured using Nile red as a fluorescence probe.

When the concentration of the PEG_{5k}-(Fmoc-NLG)₂ reached the CMC, the fluorescence intensity of Nile red would change dramatically due to the transfer of Nile red from polar microenvironment to nonpolar surroundings caused by the encapsulation into the core of our micellar system. The CMC of PEG_{5k}-(Fmoc-NLG)₂ was determined to be 0.66 μM by crossover point at the low concentration range, which was similar to our previous carrier PEG_{2k}-Fmoc-NLG (0.737 μM). The relatively low CMC may render the PEG_{5k}-(Fmoc-NLG)₂ micelles stable upon dilution *in vivo*.

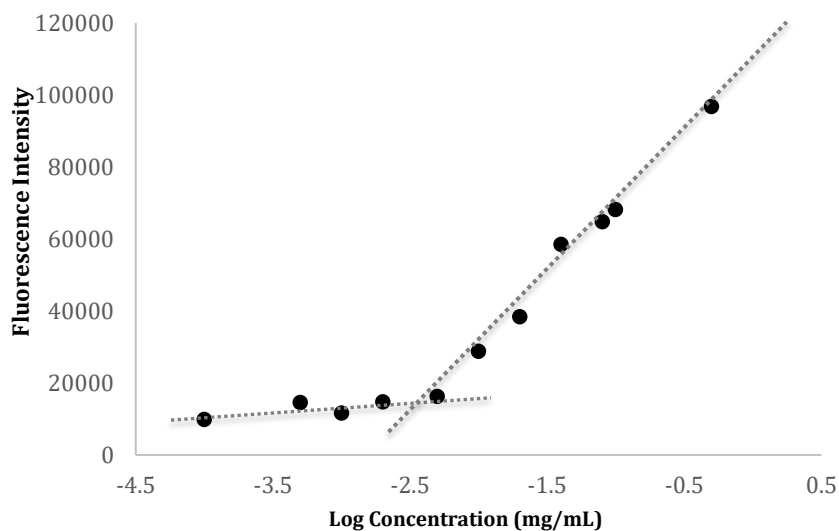


Figure 8. Critical micelle concentration (CMC) of PEG_{5k}-(Fmoc-NLG)₂ micelle.

3.5.4 Kynurenine Inhibition Measurement of PEG_{5k}-(Fmoc-NLG)₂ Conjugate.

Hela cells can be induced by proinflammatory cytokines to express endogenous IDO, which consequently leads to production and secretion into culture medium of kynurenine. So we determine the ability of free NLG and PEG_{5k}-(Fmoc-NLG)₂ conjugate to inhibit the kynurenine production in recombinant ifn- γ -treated Hela cells. Figure 9 shows that free NLG inhibited kynurenine production in a concentration-dependent manner. PEG_{5k}-(Fmoc-NLG)₂ conjugate was also effective in inhibiting the kynurenine production but less potently compared to free NLG.

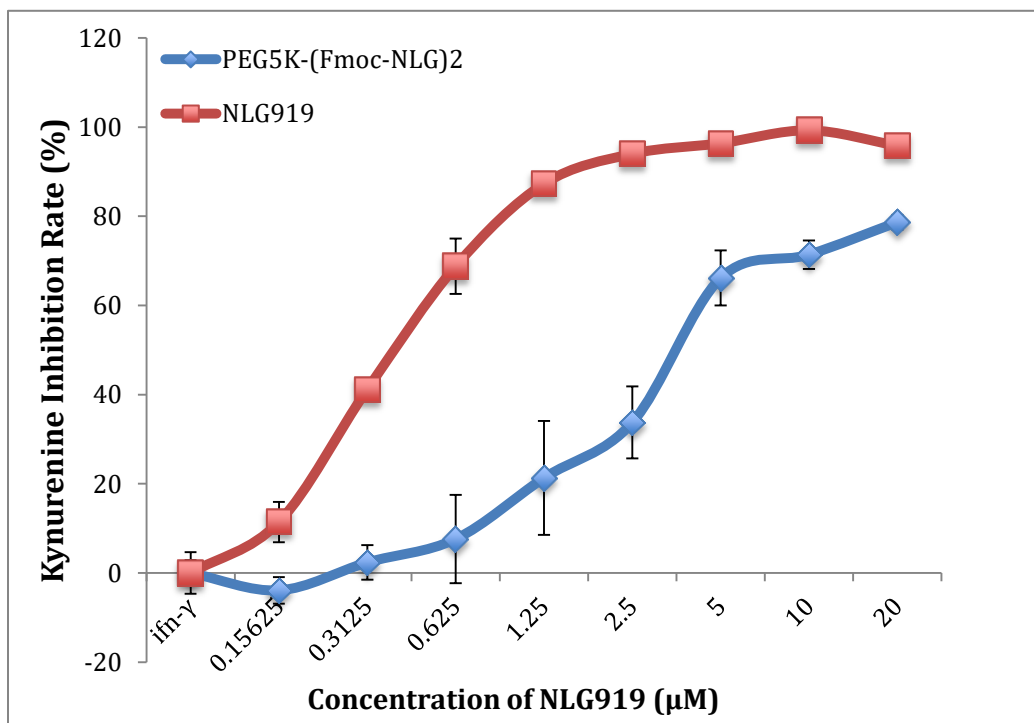


Figure 9. NLG and PEG_{5k}-(Fmoc-NLG)₂ conjugate potently inhibit kynurenine production at a dose-dependent manner in ifn- γ -treated Hela cells. Concentration of ifn- γ = 50 ng/mL. The experiment was performed in triplicate and all values are mean \pm Standard Deviation.

3.5.5 *In Vitro* Cytotoxicity of Drug-loaded PEG_{5k}-(Fmoc-NLG)₂ Micelles.

The anti-tumor activities of PTX/PEG_{5k}-(Fmoc-NLG)₂, IMA/PEG_{5k}-(Fmoc-NLG)₂ and (PTX+IMA)/PEG_{5k}-(Fmoc-NLG)₂ micelles were examined in 4T1.2, PANC-2, MCF-7 and PC-3 tumor cells and compared with Taxol. As shown in figure 10, Taxol inhibited the proliferation of several cancer cells at a concentration dependent manner. Delivery of PTX or PTX plus IMA via PEG_{5k}-(Fmoc-NLG)₂ micelles showed similar levels of cytotoxicity in all these four cancer cells, suggesting lack of synergy between the two drugs upon codelivery by PEG_{5k}-(Fmoc-NLG)₂ micelles.

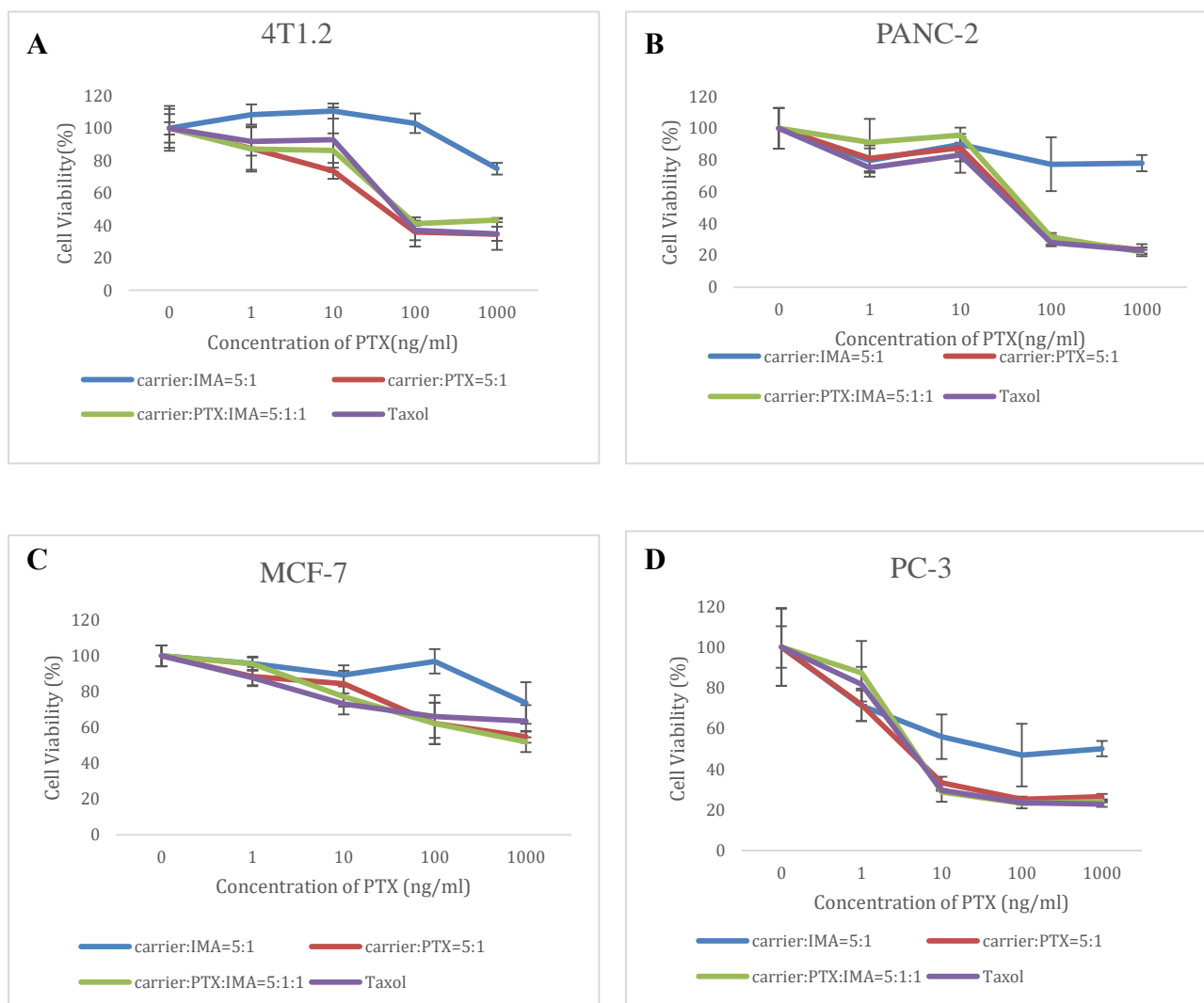


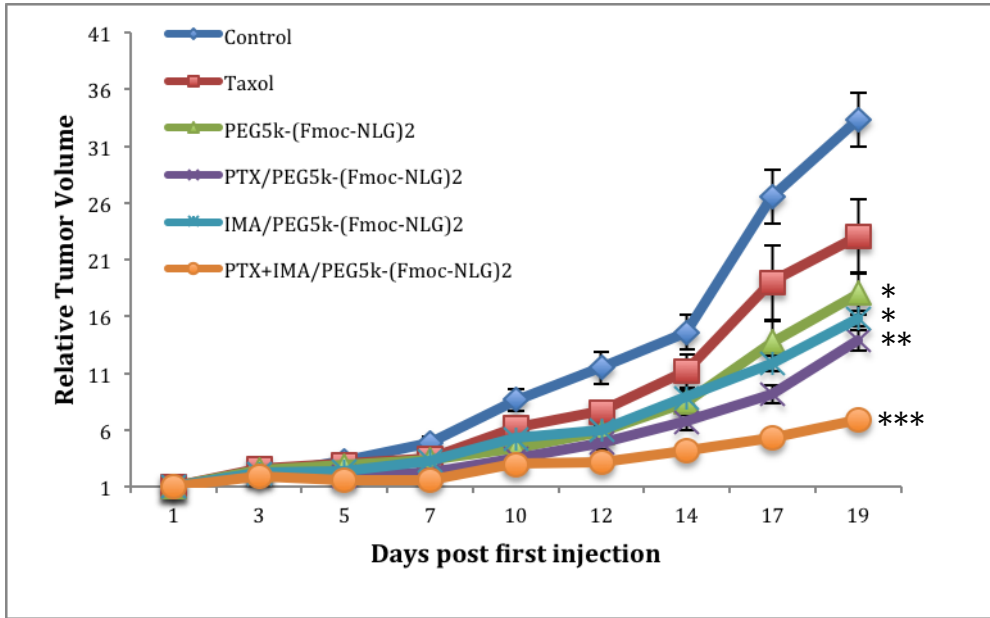
Figure 10. Cytotoxicity of PTX-loaded PEG_{5k}-(Fmoc-NLG)₂, IMA-loaded PEG_{5k}-(Fmoc-NLG)₂ and PTX+IMA-loaded PEG_{5k}-(Fmoc-NLG)₂ micelles in comparison to Taxol formulation in various types of tumor cells including (A) 4T1.2, (B) PANC-2, (C) MCF-7 and (D) PC-3. The experiment was performed in triplicate and all values are mean ± Standard Deviation.

3.6 *In Vivo* Therapeutic Study

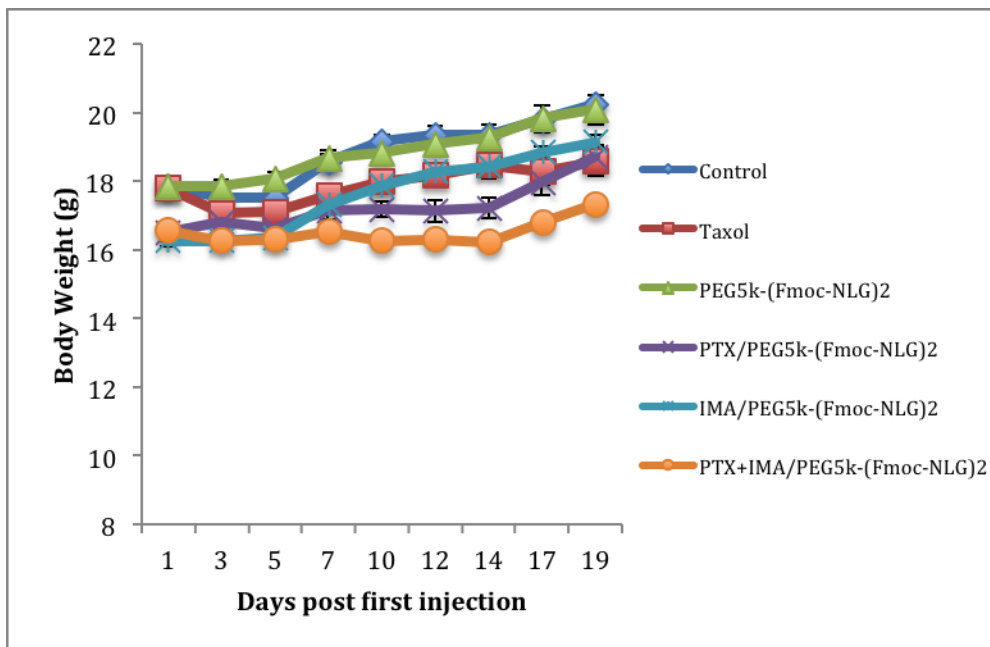
The antitumor activity of PTX-, IMA- and (PTX+IMA)-loaded PEG_{5k}-(Fmoc-NLG)₂ micelles was evaluated in an aggressive breast cancer model (BALB/c bearing 4T1.2).

Since 4T1.2 grows at a very high proliferation rate, the PBS-treated control group displayed a rapid increase in tumor size during the experiment period. Both Taxol formulation (10mg PTX/kg) and drug-free PEG_{5k}-(Fmoc-NLG)₂ micelles showed modest effect in inhibiting the tumor growth. In contrast, PTX formulated in our PEG_{5k}-(Fmoc-NLG)₂ micelles exhibited a much more potent antitumor activity at the same dose. IMA (20 mg/kg) formulated in PEG_{5k}-(Fmoc-NLG)₂ micelles also showed a level of antitumor activity that was slightly higher than that of carrier alone. However, the most pronounced antitumor effect was obtained in the group of PTX and IMA co-delivery of PTX and IMA micelles group. In addition to significant tumor growth inhibition, the tumor in one mouse completely disappeared at the end of the treatment. All of the formulations were well tolerated and there were no significant differences in body weights among the different groups.

A



B



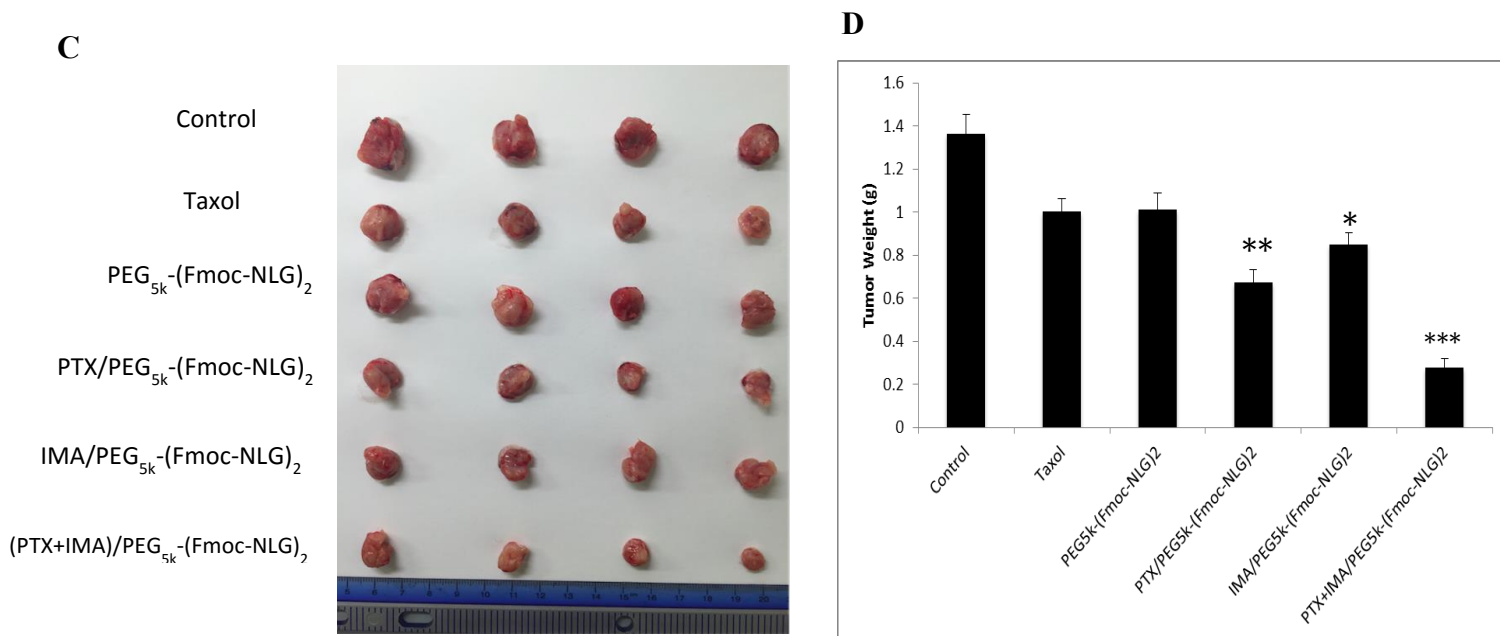


Figure 11. (A) *In vivo* therapeutic study of drug free PEG_{5k}-(Fmoc-NLG)₂, PTX-loaded PEG_{5k}-(Fmoc-NLG)₂, IMA-loaded PEG_{5k}-(Fmoc-NLG)₂ and PTX+IMA-loaded PEG_{5k}-(Fmoc-NLG)₂ micelles in comparison to Taxol formulation on 4T1.2 bearing BALB/c mice model. n=4-5 each group. Injection was given on day 0, 2, 4, 7 and 10 respectively. (B) Changes of body weight in mice that received different treatments. (C) Observation of tumor size from each group. (D) Average tumor weight from each group. Significance determined by one-way ANOVA with Fisher's post hoc test; p* < 0.05, p** < 0.01, p*** < 0.001.

All values are mean ± S.E.M

3.7 RT-PCR Analysis of IDO Transcripts from tumor tissues.

The tumor tissues were collected at the end of the experiments and subjected to RT-PCR analysis of IDO mRNA expression. As shown in Figure 12, Taxol, PEG_{5k}-(Fmoc-NLG)₂ micelles and PTX formulated micelles all showed induction effect on IDO expression while IMA formulated micelles and PTX+IMA co-loaded micelles all resulted in lower IDO expression level.

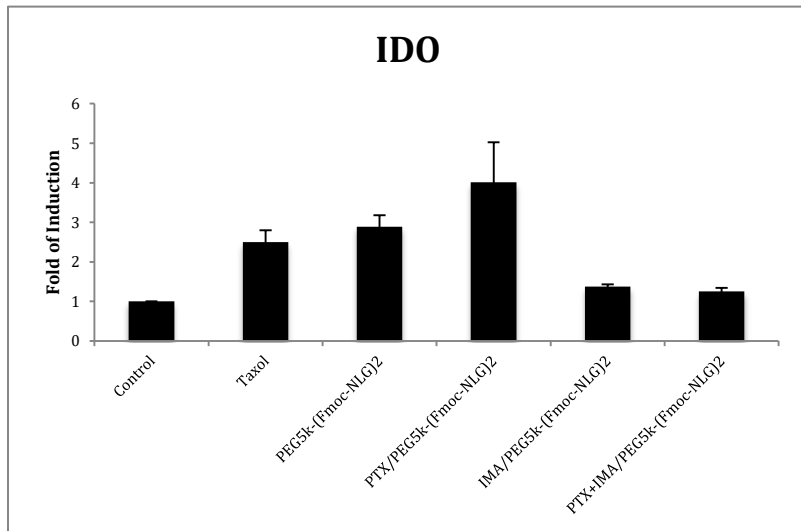


Figure 12. qRT-PCR analysis showing IDO mRNA from mouse 4T1.2 tumor tissues (n=4-5 each group).

All values are mean \pm S.E.M

4. DISCUSSION

Immunochemotherapy that combines the chemotherapeutic agents with the immune checkpoint inhibitors represents one of the attractive strategies for cancer treatment. We have recently developed a PEG-NLG-based dual functional carrier (PEG_{2k}-Fmoc-NLG) that facilitates co-delivery of a chemotherapeutic agent (e.g., PTX) and NLG, a potent inhibitor of IDO. However, NLG inhibits IDO at the enzymatic level and this may activate the feedback mechanisms, which may lead to increased expression of IDO at transcriptional level and limit the overall efficacy of the treatment. Indeed, we showed that NLG treatment led to significant upregulation of IDO expression following treatment of the carrier alone. Interestingly, we have shown that chemotherapeutic agents such as PTX, DOX and DAS can also induce the expression of the IDO mRNA, particularly in combination with ifn- γ . The mechanism of ifn- γ induction by PTX and other anticancer agents is not clear at present. However, we showed PTX can trigger the ifn- γ response in tumor cells, which may subsequently contribute to the induction of the expression of IDO mRNA.

Another interesting observation from this study is that the induction of IDO mRNA expression by PTX alone or in combination with ifn- γ , was significantly inhibited by IMA. We hypothesized that co-delivery of PTX and IMA by a PEG-NLG-based carrier shall represent a more effective strategy through inhibiting IDO at both enzymatic and transcriptional levels. Accordingly, an improved PEG-NLG-based carrier, PEG_{5k}-(Fmoc-NLG)₂ was synthesized to facilitate co-delivery of PTX and IMA. PEG_{5k}-(Fmoc-NLG)₂ was more effective than PEG_{2k}-Fmoc-NLG in co-formulating PTX and IMA likely due to

the increased size of the hydrophobic pocket. The increased number of Fmoc may also contribute to the more effective carrier/drug interaction.

Co-delivery of IMA and PTX via PEG_{5k}-(Fmoc-NLG)₂ micelles led to a significant improvement in antitumor activity in vivo compared to IMA/PEG_{5k}-(Fmoc-NLG)₂ or PTX/PEG_{5k}-(Fmoc-NLG)₂. The improvement in therapeutic efficacy in the combination group is unlikely due to an additive effect from direct killing of tumor cells by each agent alone as the two agents showed no synergy in the in vitro cytotoxicity. This is likely attributed to a more drastic overall inhibition of IDO as supported by the significantly lower levels of IDO mRNA in the combination group compared to the group treated with PTX/PEG_{5k}-(Fmoc-NLG)₂. More studies are needed to better understand the underlying mechanism.

BIBLIOGRAPHY

- 1 Rawat, M., Singh, D., Saraf, S. & Saraf, S. Nanocarriers: promising vehicle for bioactive drugs. *Biological and Pharmaceutical Bulletin* **29**, 1790-1798 (2006).
- 2 Haag, R. & Kratz, F. Polymer therapeutics: concepts and applications. *Angewandte Chemie International Edition* **45**, 1198-1215 (2006).
- 3 Davis, M. E. & Shin, D. M. Nanoparticle therapeutics: an emerging treatment modality for cancer. *Nature reviews Drug discovery* **7**, 771-782 (2008).
- 4 Nie, S., Xing, Y., Kim, G. J. & Simons, J. W. Nanotechnology applications in cancer. *Annu. Rev. Biomed. Eng.* **9**, 257-288 (2007).
- 5 Torchilin, V. P. Micellar nanocarriers: pharmaceutical perspectives. *Pharmaceutical research* **24**, 1-16 (2007).
- 6 Zitvogel, L., Apetoh, L., Ghiringhelli, F. & Kroemer, G. Immunological aspects of cancer chemotherapy. *Nat Rev Immunol* **8**, 59-73, doi:10.1038/nri2216 (2008).
- 7 Bracci, L., Schiavoni, G., Sistigu, A. & Belardelli, F. Immune-based mechanisms of cytotoxic chemotherapy: implications for the design of novel and rationale-based combined treatments against cancer. *Cell Death Differ* **21**, 15-25, doi:10.1038/cdd.2013.67 (2014).
- 8 Kroemer, G., Galluzzi, L., Kepp, O. & Zitvogel, L. Immunogenic cell death in cancer therapy. *Annu Rev Immunol* **31**, 51-72, doi:10.1146/annurev-immunol-032712-100008 (2013).
- 9 Pardoll, D. M. The blockade of immune checkpoints in cancer immunotherapy. *Nat Rev Cancer* **12**, 252-264, doi:10.1038/nrc3239 (2012).
- 10 Tentori, L., Lacal, P. M. & Graziani, G. Challenging resistance mechanisms to therapies for metastatic melanoma. *Trends Pharmacol Sci* **34**, 656-666, doi:10.1016/j.tips.2013.10.003 (2013).
- 11 Topalian, S. L., Drake, C. G. & Pardoll, D. M. Immune checkpoint blockade: a common denominator approach to cancer therapy. *Cancer Cell* **27**, 450-461, doi:10.1016/j.ccell.2015.03.001 (2015).
- 12 Korman, A. J., Peggs, K. S. & Allison, J. P. Checkpoint blockade in cancer immunotherapy. *Advances in immunology* **90**, 297-339 (2006).
- 13 Prendergast, G. C. *et al.* Indoleamine 2,3-dioxygenase pathways of pathogenic inflammation and immune escape in cancer. *Cancer Immunol Immunother* **63**, 721-735, doi:10.1007/s00262-014-1549-4 (2014).
- 14 Yoshida, R., Urade, Y., Tokuda, M. & Hayaishi, O. Induction of indoleamine 2, 3-dioxygenase in mouse lung during virus infection. *Proceedings of the National Academy of Sciences* **76**, 4084-4086 (1979).
- 15 Yoshida, R. & Hayaishi, O. Induction of pulmonary indoleamine 2, 3-dioxygenase by intraperitoneal injection of bacterial lipopolysaccharide. *Proceedings of the National Academy of Sciences* **75**, 3998-4000 (1978).
- 16 Pfefferkorn, E. Interferon gamma blocks the growth of *Toxoplasma gondii* in human fibroblasts by inducing the host cells to degrade tryptophan. *Proceedings of the National Academy of Sciences* **81**, 908-912 (1984).

- 17 Munn, D. H. *et al.* Prevention of allogeneic fetal rejection by tryptophan catabolism. *Science* **281**, 1191-1193 (1998).
- 18 Mellor, A. L. & Munn, D. H. IDO expression by dendritic cells: tolerance and tryptophan catabolism. *Nature Reviews Immunology* **4**, 762-774 (2004).
- 19 Adams, J. L., Smothers, J., Srinivasan, R. & Hoos, A. Big opportunities for small molecules in immuno-oncology. *Nat Rev Drug Discov* **14**, 603-622, doi:10.1038/nrd4596 (2015).
- 20 Mellor, A. L. & Munn, D. H. IDO expression by dendritic cells: tolerance and tryptophan catabolism. *Nat Rev Immunol* **4**, 762-774, doi:10.1038/nri1457 (2004).
- 21 Chen, W. IDO: more than an enzyme. *Nature immunology* **12**, 809-811 (2011).
- 22 Sheridan, C. IDO inhibitors move center stage in immuno-oncology. *Nat Biotechnol* **33**, 321-322, doi:10.1038/nbt0415-321 (2015).
- 23 Zhang, X. *et al.* Targeted delivery of anticancer agents via a dual function nanocarrier with an interfacial drug-interactive motif. *Biomacromolecules* **15**, 4326-4335, doi:10.1021/bm501339j (2014).
- 24 Gao, X. *et al.* Nanoassembly of surfactants with interfacial drug-interactive motifs as tailor-designed drug carriers. *Molecular pharmaceuticals* **10**, 187-198 (2012).
- 25 Iqbal, N. & Iqbal, N. Imatinib: a breakthrough of targeted therapy in cancer. *Chemotherapy research and practice* **2014** (2014).
- 26 Balachandran, V. P. *et al.* Imatinib potentiates antitumor T cell responses in gastrointestinal stromal tumor through the inhibition of Ido. *Nat Med* **17**, 1094-1100, doi:10.1038/nm.2438 (2011).
- 27 Zitvogel, L., Rusakiewicz, S., Routy, B., Ayyoub, M. & Kroemer, G. Immunological off-target effects of imatinib. *Nature reviews. Clinical oncology*, doi:10.1038/nrclinonc.2016.41 (2016).
- 28 Campia, I. *et al.* An Autocrine Cytokine/JAK/STAT-Signaling Induces Kynurenine Synthesis in Multidrug Resistant Human Cancer Cells. *PloS one* **10**, e0126159, doi:10.1371/journal.pone.0126159 (2015).
- 29 Jurgens, B., Hainz, U., Fuchs, D., Felzmann, T. & Heitger, A. Interferon-gamma-triggered indoleamine 2,3-dioxygenase competence in human monocyte-derived dendritic cells induces regulatory activity in allogeneic T cells. *Blood* **114**, 3235-3243, doi:10.1182/blood-2008-12-195073 (2009).